

Maderas. Ciencia y tecnología

ISSN: 0717-3644 ISSN: 0718-221X

Universidad del Bío-Bío

Hu, Wengang; Yu, Runzhong

Mechanical and acoustic characteristics of four wood species subjected to bending load

Maderas. Ciencia y tecnología, vol. 25, 39, 2023

Universidad del Bío-Bío

DOI: https://doi.org/10.4067/s0718-221x2023000100437

Available in: https://www.redalyc.org/articulo.oa?id=48575202036



Complete issue

More information about this article

Journal's webpage in redalyc.org



Scientific Information System Redalyc

Network of Scientific Journals from Latin America and the Caribbean, Spain and Portugal

Project academic non-profit, developed under the open access initiative

ISSN impresa 0717-3644 ISSN online 0718-221X

DOI: 10.4067/s0718-221x2023000100439

MECHANICAL AND ACOUSTIC CHARACTERISTICS OF FOUR WOOD SPECIES SUBJECTED TO BENDING LOAD

Wengang Hu^{1,2,}

https://orcid.org/0000-0001-8077-6324

Runzhong Yu²

https://orcid.org/0009-0007-3913-0573

ABSTRACT

The mechanical and acoustic properties of four commonly used wood species, including Populus tomentosa (Poplar), Swietenia mahagoni (Mahogany), Fagus orientalis (Beech), and Fraxinus excelsior (Ash) wood were investigated through using three-point bending and notched bending tests synchronizing with power spectrum analysis method and fractal dimension theory. The results showed that the bending modulus of elasticity and modulus of rapture changed in the same trend with the order ranging from high to low was ash, beech, poplar, and mahogany, successively. The brittle fracture occurred in mahogany samples and ductile fracture raised in the other three wood species. Positive proportional correlation was observed between maximum acoustic pressure and fractal dimension of power spectrum regardless of seeing four wood species as independent or population samples. The failure modes can be identified by amplitude-frequency curve and fractal dimension of power spectrum with following laws: the peak value in amplitude-frequency curve and fractal dimension of power spectrum were relatively higher when a single crack developed at latewood; for crack developed at earlywood, only one peak was observed in power amplitude-frequency curves, and the corresponding fractal dimension of power spectrum was smaller than the that of latewood; in case of failure modes with two cracks developed at earlywood, there are two peaks in amplitude-frequency curve and the fractal dimension of power spectrum was between those of single crack developed at earlywood and latewood. The vibrational properties of the four wood species can be characterized through using power spectrum analysis method and notched bending test method can be used to distinguish the failure modes of samples.

Keywords: Fractal dimension, mechanical properties, notched bending, vibrational characteristic, wood species.

¹Nanjing Forestry University. Co-Innovation Center of Efficient Processing and Utilization of Forest Resources. Nanjing, China.

²Nanjing Forestry University. Department of Furniture Design. College of Furnishings and Industrial Design. Nanjing, China.

*Corresponding author: hwg@njfu.edu.cn

INTRODUCTION

Acoustic emission (AE) is the emission of sound waves in the audible and ultrasonic range, which is caused be microscopic fractures, friction of fracture surfaces, outflow of liquids, transport process in capillaries of other effects (Niemz *et al.* 2022). The AE has been studied for nearly half a century in the field of wood and wood-based materials. The AE technique includes determining the physical and mechanical properties of wood, as well as grading, drying, and detecting defects of wood based on the AE of wood when subjected to loads (Hu *et al.* 2021a, Zhao *et al.* 2020). The AE has been widely used in healthy monitoring of wood constructions including wood timber, shear wall, and other component of wood buildings and products (Yin *et al.* 2021). The focus of AE is the investigation of the relationships between structure and properties of wood. However, the vibrational properties of wood were rarely investigated.

It is known that AE in wood can appear as a result of mechanical stresses caused by mechanical, external loading or wood-internal sorptive stresses (Raczkowski *et al.* 1994). So far, many publications (Krajewski *et al.* 2020, Yan *et al.* 2022, Wu *et al.* 2021, Nasir *et al.* 2019, Niu and Huang 2022, Tang *et al.* 2022) had reported the basic knowledge of AE generated by external loading and AE applied to monitor the AE generated by wood-internal sorptive stresses in wood products and structures. Ozyhar *et al.* (2013) determined the moisture-dependent elastic characteristics of beech wood by means of ultrasonic waves.

Researchers have tried to obtain more accurate AE signals to know the position and details of cracks in wood and wood constructions. However, AE characteristic signals of wood are affected by many factors, such as wood species (Perrin *et al.* 2019, Xu *et al.* 2020, Ansell 1982, Lin *et al.* 2022, Liu *et al.* 2023), moisture content (Sato *et al.* 1984, Fu *et al.* 2021), density (softwood and hardwood) (Ansell 1982, Reiterer *et al.* 2000, Chen *et al.* 2006), wood grains (Brémaud *et al.* 2011, Boccacci *et al.* 2022), loading types (Chen *et al.* 2006, Ohuchi *et al.* 2011) and the distance between the AE source and the transducers (Lukomski *et al.* 2017, Pan *et al.* 2022, Zhao *et al.* 2022, Zhu *et al.* 2022). Most studies were mainly focused on how these factors influenced AE characteristic signals and their relationships with mechanical properties of wood (Rescalvo *et al.* 2020). The most important factors influencing AE of wood are the structure (density, fiber length, particle geometry, type, and percentage of adhesive, etc.), the moisture content, and the history (e.g., fungal infections or insect attack, mechanical or climate pre-stress) of wood and wood-based material (Niemz *et al.* 2022).

All above studies indicated that: 1) ratio of earlywood to latewood had significant effect on AE signals when subjected to tensile load (Ansell 1982); 2) AE signals of wood decreased in high moisture content (Sato et al. 1984); 3) AE counts of softwoods were higher than those of hardwoods when cracked in mode I compact tension tests, while in torsion load condition, opposite results were obtained (Sato et al. 1984), which suggested that loading types seriously influenced AE events. In addition, Perrin et al. (2019) investigated the effects of wood species on AE signals under four-point bending load condition, which reported that unique AE signal appeared for each kind of wood species indicating that the more diverse the wood species was, the more characteristic the AE signal was. This contributes to classify the different wood species.

Above research confirmed that AE signal has potential in evaluating wood mechanical properties. However, there are still many aspects of AE properties unknown. The aim of this study was to obtain and compare the AE characteristics of four commonly used wood species. In this study, the maximum acoustic pressure and power spectrum of four commonly used wood species under three-point bending load condition using notched bending samples. Specifically,

1) the physical and mechanical properties of the four wood species were studied; 2) the mechanical and acoustic characteristics of the four wood species were determined using notched bending test method; 3) failure modes of notched bending samples were analyzed based on fractal dimension theory; 4) the relationship between vibrational characteristics and fractal dimension was fitted.

MATERIALS AND METHODS

Materials

The four wood species used in this study were Poplar (*Populus tomentosa* Carrière), Mahogany (*Swietenia mahagoni* (L.) Jacq.), Beech (*Fagus orientalis* Lipsky), and Ash (*Fraxinus excelsior* L.). All above wood lumbers were bought from local commercial wood supplier (Nanjing, China) and stored in the woodshop of Nanjing Forestry University for more than 12 months and reached air dry condition.

Specimen preparation

Figure 1 shows the dimensions of the samples used in this study. All these samples were cut from full-size lumbers of each species. The samples for three-point bending tests measured 300 mm \times 20 mm \times 20 mm (length \times width \times thickness) according to the ASTM D4761-19 (2019). The dimensions of sample for notched bending test were the same with those of three-point bending test except a notch measured 5 mm \times 10 mm \times 20 mm (height \times width \times depth) at the middle of length, and 1 mm initial cracks at the notch corners were made using a knife. Among these four wood species, the boundary of earlywood and latewood of ash wood were clear. Therefore, for ash wood samples, the notched bending test samples with initial cracks at earlywood and latewood.

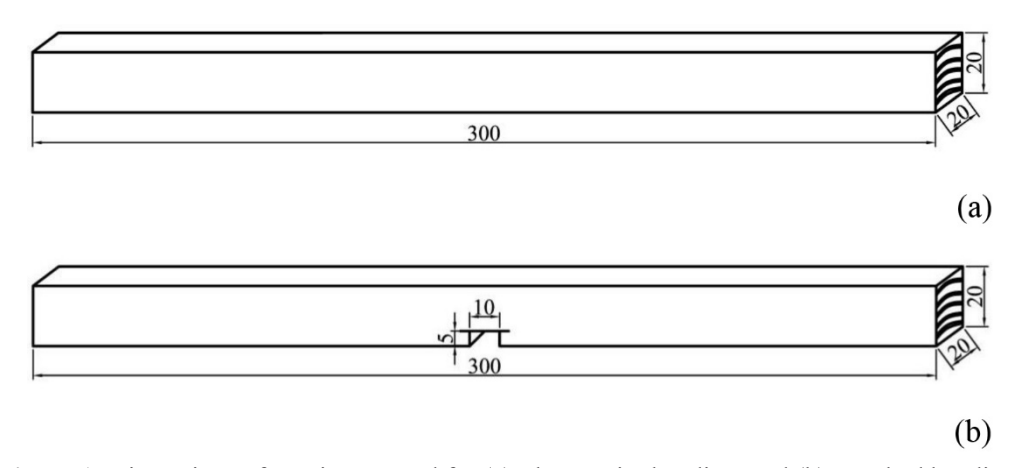


Figure 1: Dimensions of specimens used for (a) Three-point bending, and (b) Notched bending.

Experimental design

Table 1 shows the experimental design, which indicates that there are 108 samples prepared in this study with 12 replications for each combination of wood species and testing methods. After bending tests, the clear samples measured $20 \text{ mm} \times 20 \text{ mm} \times 20 \text{ mm}$ were cut at the non-destruction parts for measurements of specific gravity (SG) and moisture content (MC) with 10 replications for each species.

_		•		•
	Testing methods			
Wood species	Three-point	Notched		SG and
	bending	bending		MC
Poplar (Populus tomentosa)	12	12		10
Mahogany (Swietenia mahagoni)	12	12		10
Beech (Fagus orientalis)	12	12		10
Ash (Fraxinus	12	Earlywood	10	10
excelsior)	12	Latewood	10	10

Table 1: Arrangement of samples tested in this study.

Testing methods

Three-point bending

The three-point bending tests were conducted according to ASTM D4761-19 (2019). The load was controlled by displacement with a loading rate 5 mm/min. The bending modulus of elasticity (MOE) and the modulus of rapture (MOR) of the four wood species were calculated using Equation 1 and Equation 2, respectively. The first loading point was 200 N, and second loading point was 700 N, which were selected to ensure the wood kept in elastic stage. The MOE can be calculated according to Equation 1. Then the load continued until samples completely failed. The MOR is available using Equation 2.

$$E = \frac{\Delta P l^3}{4\Delta f b h^2}$$
 (1)

Where E is bending modulus of elasticity (MPa); is bending modulus of rapture (MPa); ΔP is change of load in elastic range (N); Δf is change of deflection corresponding to ΔP (mm); l, b and h are length, width, and height (mm) of samples, respectively; P_{\max} is the ultimate load when samples fracture (N).

Notched bending

Figure 2 shows the setup for the notched bending tests and vibrational properties tests. The loading condition was the same with that of three-point bending test, the span was 240 mm. Meanwhile, a non-touched microphone sensor (with a pre-amplifier built in) was set in front of the notched corner with 5 mm (Figure 2) used to record the vibrational signal generated during the cracks propagation when subjected to the notched bending load. The universal testing machine did not stop loading until reaching the maximum load. The universal testing machine and computer recorded the load and deflection data, and the FFT analyzer (CF9200, ONOSOKKI, Japan) recorded the vibrational signals including maximum acoustic pressure and power spectrum. The specific settings of the FFT were that 1) the sample frequency ranged from 0 kHz to 4 kHz with a sample point of 2018; 2) the threshold of the microphone was 1 Pa to filter environmental noise. The main testing procedure was that: 1) turn on the FFT analyzer and set the parameters according to above descriptions; 2) start loading until sample fail with a loading speed of 5 mm/min controlled by displacement; 3) output the data, *i.e.*, time, deflection, and load, from the universal testing machine, and vibrational signals, *i.e.*, frequency, amplitude, and acoustic pressure, were also outputted from the FFT analyzer.

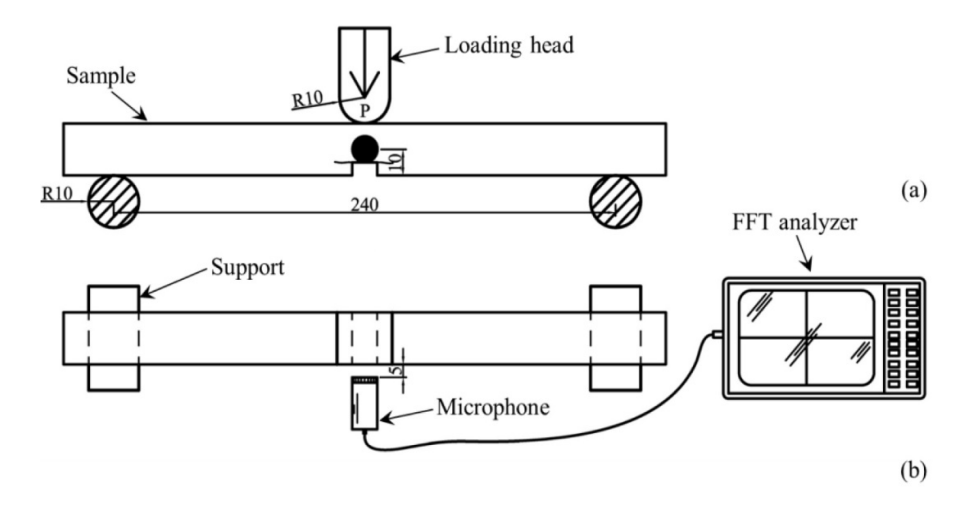


Figure 2: Setup for testing acoustic emission properties when subjected to notched bending load: (a) Front view; (b) Top view.

Specific gravity and moisture content

After finishing the three-point bending tests and notched bending tests, the SG and MC were measured using the samples cut from the tested three-point samples according to the ASTM D2395-17 (2022) and the ASTM D4442-20 (2020), respectively.

Statistical analysis

The basic physical, mechanical properties, and acoustic characteristics of the four types of wood species were analyzed using analysis of variance (ANOVA) general linear method (GLM) procedure. Mean comparisons using the protected least significant difference (LSD) multiple comparison procedure was conducted if any significant was identified. All these analyses were performed at 5% significance level using the SPSS 22.0 (IBM 2013). Fractal dimensions were calculated using the Fraclab 2.2 toolbox (INRIA 2017) built in the MATLAB R2014a (MathWorks 2014). The specific calculation procedure of fractal dimensions of power spectrum followed our former work (Hu *et al.* 2021b).

RESULTS AND DISCUSSION

Basic physical and mechanical properties

Figure 3 shows the typical load and deflection curves of the four wood species when subjected to threepoint bending load, which indicates that the failure modes of ash, beech and poplar are ductile, and that of mahogany is nearly brittle. Table 2 further shows the mean comparisons of basic physical (SG and MC) and mechanical properties (ultimate load, MOE, and MOR) of all evaluated wood species. All testing results of dependent variables evaluated were in normality distributions. Significant differences of SG exist between the four wood species. The specific order of SG from high to low is Ash (Fraxinus excelsior L.), Beech (Fagus orientalis Lipsky), Mahogany (Swietenia mahagoni (L.) Jacq.), and Poplar (Populus tomentosa Carrière). In case of MC, Ash (Fraxinus excelsior L.) wood had significantly higher MC than Beech (Fagus orientalis Lipsky) and Mahogany (Swietenia mahagoni (L.) Jacq.) followed by Poplar (Populus tomentosa Carrière), but the difference between Beech (Fagus orientalis Lipsky) and Mahogany (Swietenia mahagoni (L.) Jacq.) was not significant. The values of all mechanical properties of the four wood species had the same trends that Ash (Fraxinus excelsior L.) and Beech (Fagus orientalis Lipsky) had significantly greater values than those of Poplar (Populus tomentosa Carrière) and Mahogany (Swietenia mahagoni (L.) Jacq.), but no significantly difference was found between Ash (Fraxinus excelsior L.) and Beech (Fagus orientalis Lipsky) wood. Here, the ultimate load, MOE, and MOR of Poplar (Populus tomentosa Carrière) were all significantly higher than Mahogany (Swietenia mahagoni (L.) Jacq.), which was opposite to the relative values of their density. This may lie to the brittle failure of Mahogany (Swietenia mahagoni (L.) Jacq.) shown in Figure 3.

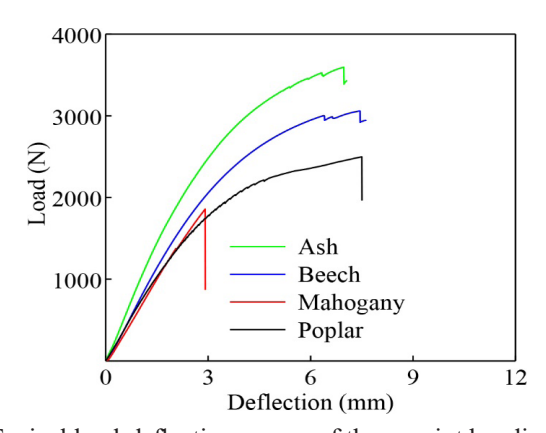


Figure 3: Typical load-deflection curves of three-point bending tests.

Wood species	Specific gravity	Moisture content (%)	Ultimate load (N)	MOE (MPa)	MOR (MPa)
Poplar (Populus tomentosa)	0,45 (9,23) D	8,64 (2,52) C	2451 (16) B	7118 (13) B	83 (14) B
Mahogany (Swietenia mahagoni)	0,65 (5,75) C	9,26 (2,20) B	1634 (24) C	6399 (16) B	59 (21) C
Beech (Fagus orientalis)	0,68 (5,53) B	9,22 (2,70) B	3051 (14) A	10958 (16) A	116 (13) A
Ash (Fraxinus excelsior)	0,74 (2,54) A	9,69 (2,37) A	3593 (11) A	11192 (12) A	120 (12) A

Table 2: Comparisons of basic physical and mechanical properties of four species evaluated.

The values in parenthesis after mean values are coefficient of variances in percentage, and four means in the same column not followed by a common letter are significant different one from another at 5% significance level.

Mechanical and acoustic properties of notched bending samples

Figure 4 shows a combination of typical load-deflection, acoustic pressure-time, and power spectrum (amplitude-frequency curve) of an ash wood sample. In theory, the acoustic pressure and power amplitude reached their peak values when the load reached the maximum value. Meanwhile, the amplitude-frequency curves indicate the energy releasing process. The greater the amplitude is, the more the energy releasing is, and the larger the area generated by fracture is. Based on the above theory, the fractal dimensions of power spectrum curve (FDPS) were used to indicate the morphology of fracture surface indirectly.

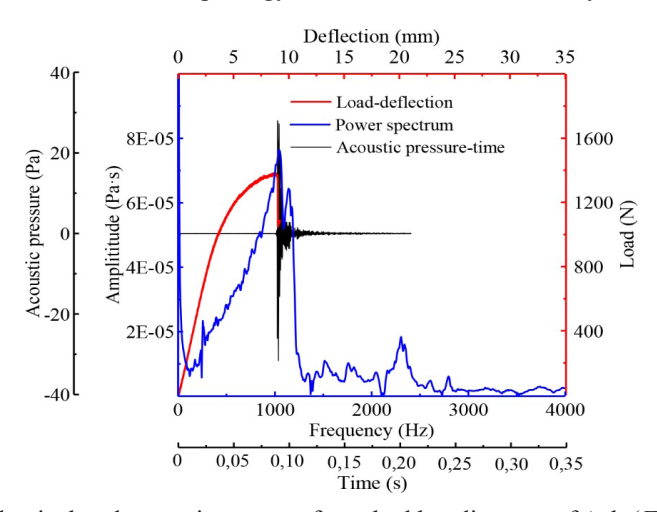


Figure 4: Typical mechanical and acoustic curves of notched bending test of Ash (*Fraxinus excelsior* L.) sample.

Table 3 shows the ultimate load, maximum acoustic pressure and FDPS of notched bending tested samples. The maximum acoustic pressure of mahogany was significantly higher than those of Poplar (*Populus tomentosa* Carrière), Beech (*Fagus orientalis* Lipsky), and Ash (*Fraxinus excelsior* L.). There were no significant differences between poplar, beech, and ash. Combining the failure modes and load-deflection curves shown in Figure 5, it can be found that the failure mode of mahogany under notched bending test was also brittle, and the other three wood species were ductile, which was consistent with three-point bending test. Above results also confirmed the results of other researchers (Lukomski *et al.* 2017) that mahogany was more

sensitive to notched corner than the other three wood species.

Table 3: Comparisons of mechanical and vibrational characteristics of notched bending samples for four wood species.

Wood species	Maximum acoustic pressure (Pa)	Ultimate load (N)	FDPS
Poplar (Populus tomentosa)	18 (34) B	746 (33) C	1,333 (6,5) A
Mahogany (Swietenia mahagoni)	24 (45) A	623 (19) C	1,270 (4,6) C
Beech (Fagus orientalis)	16 (60) B	1089 (28) B	1,282 (6,0) B
Ash (Fraxinus excelsior)	17 (41) B	1305 (13) A	1,290 (3,3) B

The values in parenthesis after mean values are coefficient of variances in percentage, and four means in the same column not followed by a common letter are significant different one from another at 5% significance level.

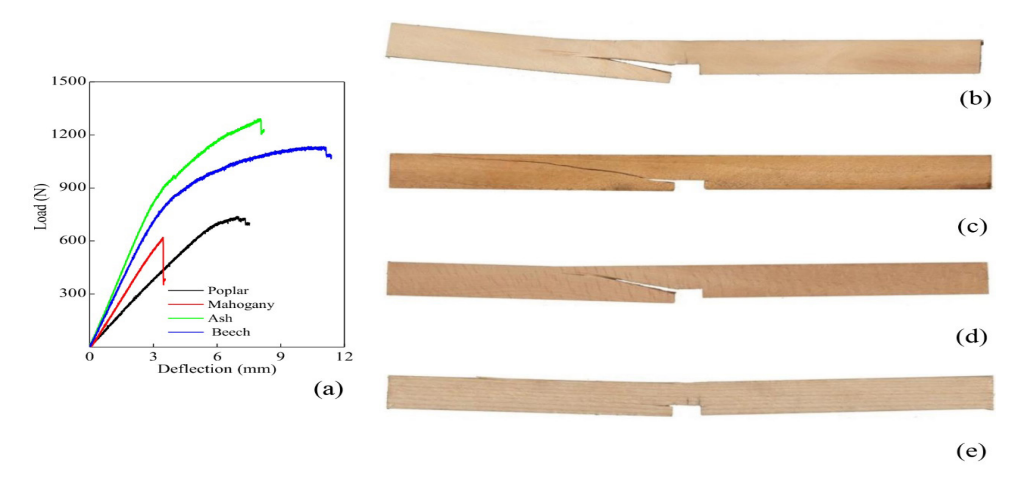


Figure 5: Failure modes of notched bending tested samples: (a) Load-deflection curves; (b) Poplar (*Populus tomentosa* Carrière); (c) Mahogany (*Swietenia mahagoni* (L.) Jacq.); (d) Beech (*Fagus orientalis* Lipsky); (e) Ash (*Fraxinus excelsior* L.).

Relationships between acoustic pressure and FDPS

For further analysis, the acoustic characteristics, Figure 6 shows the relationships between maximum acoustic pressure and FDPS fitted using linear regression method regarding each wood species as independent sample and population sample, respectively.

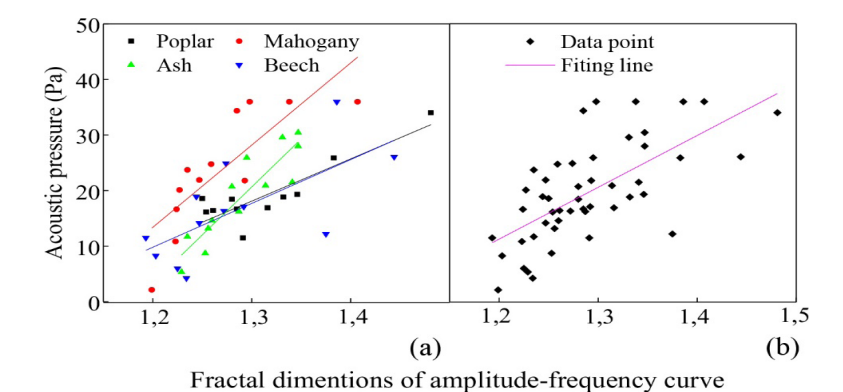


Figure 6: Relationship between maximum acoustic pressure and FDPS: (a) Independent sample; and (b) Population sample.

Table 4 shows the fitting equations and their corresponding correlation coefficients when four wood species were regarded as independent and population samples. It indicated that there were linear positive proportional relationships between maximum acoustic pressure and FDPS regardless of four wood species seen as independent or population samples, which suggested that the relationship maybe suitable to other wood species, but further studies need to be conducted to confirm it. Ash wood had the highest correlation coefficient of 0,904 among the four wood species, which owned to that the grains of ash wood samples are straight during samples preparation. The correlation coefficients of the other three wood species were all bigger than 0,76 which satisfied the engineering application (Zhou et al. 2022a, Zhou et al. 2022b, Tao and Yan 2022).

Failure modes of notched ash wood samples

Figure 7 shows the typical failure modes and their corresponding amplitude-frequency curves of ash wood samples when subjected to notched bending load, which indicates that there are three types of failure modes including single crack at latewood (Figure 7a), single crack at earlywood (Figure 7b), and double cracks at earlywood (Figure 7c).

Table 4: Fitting equations and correlation coefficients of acoustic pressure-FDPS lines.

S	ample	Fitting equation	Correlation coefficient	p
	Poplar (Populus tomentosa)	<i>y</i> =75,9676 <i>x</i> -80,649	0,877	0,0207
Independent sample	Mahogany (Swietenia mahagoni)	<i>y</i> =147,8792 <i>x</i> -164,057	0,810	0,0014
	Beech (Fagus orientalis)	<i>y</i> =172,6187 <i>x</i> -203,754	0,904	2,199e-5
	Ash (Fraxinus excelsior)	<i>y</i> =78,8380 <i>x</i> -203,754	0,768	0,01536
Population sample		<i>y</i> =93,1628 <i>x</i> -100,522	0,767	2,215e-7

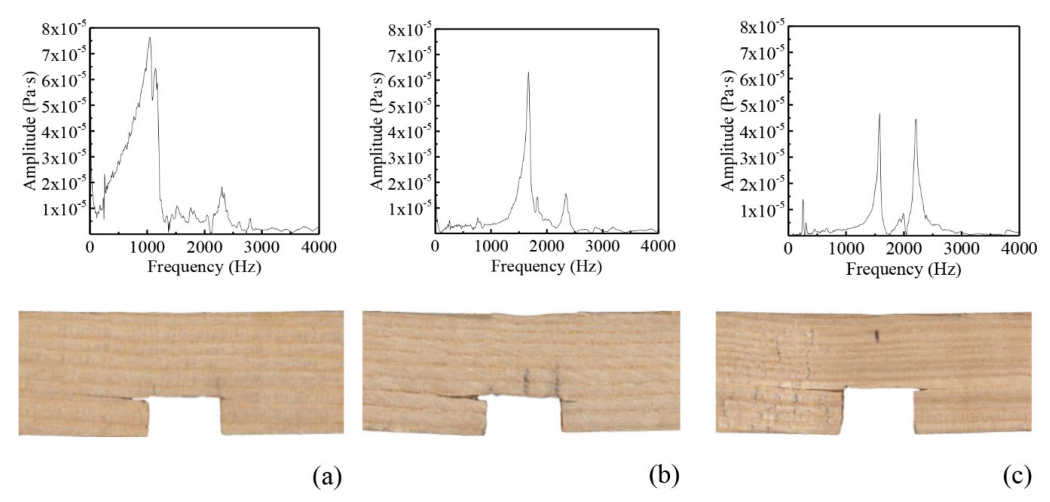


Figure 7: Typical failure modes of notched ash wood samples (a) Single crack located at latewood, (b) Single crack located at earlywood, and (c) Double cracks located at earlywood.

Table 5 shows the mean maximum amplitude and FDPS of the ash wood samples corresponding to three typical failure modes, which indicates that the maximum amplitude and FDPS values of ash wood samples with single crack generated at latewood were greater than those of earlywood. The maximum amplitude of ash wood samples with double cracks generated at earlywood was lower than those of single cracks at earlywood, but the FDPS was slightly higher than single cracks at earlywood. Meanwhile, there were two peaks in amplitude-frequency curves when the double cracks generated at earlywood, whereas, one peak when single cracks generated. Therefore, the amplitude-frequency curves and FDPS could be indicators for predicting where and numbers of cracks generated when subjected to notched bending load. Previous study also supported this point (Hu and Zhang 2022).

Table 5: Mean comparison of power spectrum and FDPS of ash failure modes.

Failure modes	Maximum amplitude (Pa·s)	FDPS	
(a)	6,42e-5 (3,4)	1,348 (2,6)	
(b)	5,67e-5 (4,1)	1,280 (4,4)	
(c)	4,51e-5 (5,3)	1,287 (3,2)	

The values in parenthesis after mean values are coefficient of variances in percentage.

CONCLUSIONS

In this study, the mechanical properties and acoustic emission of four commonly used wood species were studied through using power spectrum analysis method (PSAM) and fractal theory. Following conclusions were drawn.

The modulus of elasticity (MOE) and modulus of rapture (MOR) of the four wood species evaluated were ash, beech, poplar, and mahogany from high to low, and MOE and MOR had the same changing trends.

Although the specific gravity of mahogany was greater than poplar, the MOE and MOR of mahogany were lower than those of poplar. Because brittle fracture was occurred to mahogany when subjected to three-point bending and notched bending loads.

Mahogany had the highest acoustic pressure among the four wood species, which indicated that brittle fracture generated higher acoustic pressures. There were positive linear proportional relationships between

four wood species and fractal dimensions of power spectrum (FDPS).

The number of peaks in acoustic pressure-frequency curve of ash wood and its FDPS could be used to predict where and number of cracks generated when subjected to notched bending load.

AUTHORSHIP CONTRIBUTIONS

W. H.: Conceptualization, Resources, Data curation, Formal analysis, Methodology, Writing - original draft, Project administration, Writing - review & editing. R. Y.: Data curation, Software, Formal analysis, Validation, Writing - original draft, Writing - review & editing.

ACKNOWLEDGEMENTS

This study was supported by Scientific Research Foundation of Metasequoia Teacher (163104060), and A Project from International Cooperation Joint Laboratory for Production, Education, Research, and Application of Ecological Health Care on Home Furnishing.

REFERENCES

- **ASTM. 2019.** Standard test methods for mechanical properties of lumber and wood-based structural materials. ASTM D4761-19. ASTM: West Conshohocken, PA, USA. https://www.astm.org/d4761-19.html
- **ASTM. 2022.** Standard test methods for specific gravity (relative density) of wood and wood-based materials. ASTM D2395-17. ASTM: West Conshohocken, PA, USA. https://www.astm.org/d2395-17r22.html
- **ASTM. 2020.** Standard test methods for direct moisture content measurement of wood and wood-base materials. ASTM D4442-20. ASTM: West Conshohocken, PA, USA. https://www.astm.org/d4442-20.html
- **Ansell, M.P. 1982.** Acoustic emission from softwoods in tension. *Wood Science and Technology* 16: 35-58. https://doi.org/10.1007/BF00351373
- **Boccacci, G.; Frasca, F.; Bertolin, C.; Siano A.M. 2022.** Influencing factors in acoustic emission detection: A literature review focusing on grain angle and high/low tree ring density of scots pine. *Applied Sciences* 12: e859. https://doi.org/10.3390/app12020859
- **Brémaud, I.; Gril, J.; Thibaut, B. 2011.** Anisotropy of wood vibrational properties: dependence on grain angle and review of literature data. *Wood Science and Technology* 45:735-754. https://doi.org/10.1007/s00226-010-0393-8
- Chen, Z.; Gabbitas, B.; Hunt, D. 2006. Monitoring the fracture of wood in torsion using acoustic emission. *Journal of Materials Science* 41: 3645-3655. https://doi.org/10.1007/s10853-006-6292-6
- **Fu, W.; Guan, H.; Kei, S. 2021.** Effects of moisture content and grain direction on the elastic properties of beech wood based on experiment and finite element method. *Forests* 12: e610. https://doi.org/10.3390/f12050610
- Hu, W.; Li, S.; Liu, Y. 2021a. Vibrational characteristics of four wood species commonly used in wood products. *BioResources* 16(4): 7101-7111. https://doi.org/10.15376/biores.16.4.7101-7111
- Hu, W.; Liu, Y.; Li, S. 2021b. Characterizing mode I fracture behaviors of wood using compact tension in selected system crack propagation. *Forests* 12(10): e1369. https://doi.org/10.3390/f12101369
- Hu, W.; Zhang, J. 2022. Effect of growth rings on acoustic emission characteristic signals of southern yellow pine wood cracked in mode I. *Construction and Building Materials* 329: e127092. https://doi.org/10.1016/j.conbuildmat.2022.127092

- IBM. 2013. SPSS 22.0. Armonk: NY, USA. https://www.ibm.com/support/pages/spss-statistics-220-available-download
 - INRIA. 2017. Fraclab 2.2 toolbox. France. https://project.inria.fr/fraclab/
- Krajewski, A.; Bilski, P.; Witomski, P.; Bobinski, P.; Guz, J. 2020. The progress in the research of AE detection method of old house borer larvae (*Hylotrupes bajulus* L.) in wooden structures. *Construction and Building Materials* 256: e119387. https://doi.org/10.1016/j.conbuildmat.2020.119387
- Lin, Q.; Zhang, X.; Zhu, N.; Kusumah, S.; Umemura, K.; Zhao, Z. 2022. Preparation and investigation of an eco-friendly plywood adhesive composed of sucrose and ammonium polyphosphate. *Wood Material Science & Engineering* 17: e2121176. https://doi.org/10.1080/17480272.2022.2121176
- Liu, X.; Yang, S.; Zhang, C.; Huang, H.; Varodi, A.M. 2023. Comparative study on slow pyrolysis products of abandoned furniture materials. *BioResources* 18(1): 629-640. https://doi.org/10.15376/biores.18.1.629-640
- Lukomski, M.; Strojecki, M.; Pretzel, B.; Blades, N.; Beltran, L.; Freeman, A. 2017. Acoustic emission monitoring of micro-damage in wooden art objects to assess climate management strategies. *Insight* 59: 256-264. https://doi.org/10.1784/insi.2017.59.5.256
- MathWorks. 2014. Matlab R2014a. Natick, MA, USA. https://www.mathworks.com/company/news-room/mathworks-announces-release-2014a-of-the-matlab-and-simulink-product-families.html
- Nasir, V.; Nourian, S.; Avramidis, S.; Cool, J. 2019. Stress wave evaluation for predicting the properties of thermally modified wood using neuro-fuzzy and neural network modeling. *Holzforchung* 73: 827-838. https://doi.org/10.1515/hf-2018-0289
- Niemz, P.; Teischinger, A.; Sandberg, D. 2022. Springer Handbook of Wood Science and Technology. Springer International Publishing. https://doi.org/10.1007/978-3-030-81315-4. ISBN: 978-3-030-81314-7
- Niu, X.; Huang, T. 2022. Research on backrest modeling of Ming-style furniture with full carving using technology of eye tracking. *Journal of Forestry Engineering* 7: 200-206. https://doi.org/10.13360/j.issn.2096-1359.202108018
- Ohuchi, T.; Hermawan, A.; Fujimoto, N. 2011. Basic studies on fracture toughness of sugi and acoustic emission. *Journal of the Faculty of Agriculture, Kyushu University* 56: 99-102. https://doi.org/10.5109/19536
- Ozyhar, T.; Hering, S.; Sanabria, S.J.; Niemz, P. 2013. Determining moisture-dependent elastic characteristics of beech wood by means of ultrasonic waves. *Wood Science and Technology* 47: 329-341. https://doi.org/10.1007/s00226-012-0499-2
- Pan, P.; Yan, X.; Wang, L. 2022. Effects of thermochromic fluorane microcapsules and self-repairing waterborne acrylic microcapsules on the properties of water-based coatings on basswood surface. *Polymers* 14(12): e2500. https://doi.org/10.3390/polym14122500
- **Perrin, M.; Yahyaoui, I.; Gong, X. 2019.** Acoustic monitoring of timber structures: Influence of wood species under bending loading. *Construction and Building Materials* 208: 125-134. https://doi.org/10.1016/j.conbuildmat.2019.02.175
- Raczkowski, J.; Molinski, W.; Ranachowski, Z. 1994. Acoustic emission in fracture mechanics of wood. *Journal of Theoretical and Applied Mechanics* 32: 299-322. http://www.ptmts.org.pl/jtam/index.php/jtam/article/view/v32n2p299
- **Rescalvo, F.J.; Morillas, L.; Valverde-Palacios, I.; Gallego, A. 2020.** Acoustic emission in I-214 poplar wood under compressive loading. *European Journal of Wood and Wood Products* 78: 723-732. https://doi.org/10.1007/s00107-020-01536-7
- **Reiterer, A.; Stanzl-Tschegg, S.E.; Tschegg, E.K. 2000.** Mode I fracture and acoustic emission of softwood and hardwood. *Wood Science and Technology* 34: 417-430. https://doi.org/10.1007/s002260000056
- **Sato, K.; Kamei, N.; Fushitani, M.; Noguchi, M. 1984.** Discussion of tension fracture of wood using acoustic emission. A statistical analysis of the relationships between the characteristics of AE and fracture stress. *Mokuzai Gakkaishi* 30: 653-659. http://www.jwrs.org/english/journals/mkz-toce/mkze-30/
- Tao, Y.; Yan, X. 2022. Influence of HLB value of emulsifier on the properties of microcapsules and self-healing properties of waterborne coatings. *Polymers* 14(7): e1304. https://doi.org/10.3390/polym14071304

- **Tang, L.; Lu, L.; Guan, H. 2022.** Modern optimized design and anti-bending property of traditional corner joints. *Journal of Forestry Engineering* 7:166-173. https://doi.org/10.13360/j.issn.2096-1359.202108007
- Wu, Y.; Perrin, M.; Pastor, M.L.; Casari, P.; Gong, X.J. 2021. On the determination of acoustic emission wave propagation velocity in composite sandwich structures. *Composite Structures* 259: e113231. https://doi.org/10.1016/j.compstruct.2020.113231
- Xu, W.; Fang, X.Y.; Han, J.T.; Wu, Z.H.; Zhang, J.L. 2020. Effect of coating thickness on sound absorption property of four wood species commonly used for piano soundboards. *Wood and Fiber Science* 52: 28-43. https://doi.org/10.22382/wfs-2020-004
- Yan, X.; Li, W.; Han, Y.; Yin, T. 2022. Preparation of melamine/rice husk powder coated shellac microcapsules and effect of different rice husk powder content in wall material on properties of wood waterborne primer. *Polymers* 14(1): e72. https://doi.org/10.3390/polym14010072
- Yin, Y.; Miao, Y.; Wan, K.; Wang, X.; Zhai, X.; Liu, Z. 2021. Analysis and evaluation of wood acoustic vibration signal based on Daubechies wavelet base. *Journal of Forestry Engineering* 6: 68-75. https://doi.org/10.13360/j.issn.2096-1359.202012016
- **Zhao, Q.; Zhao, D.; Zhao, J. 2020.** Thermodynamic approach for the identification of instability in the wood using acoustic emission technology. *Forests* 11(5): e534. https://doi.org/10.3390/f11050534
- **Zhao, Z.; Zhang, X.; Lin, Q.; Zhu, N.; Gui, C.; Yong, Q. 2022.** Development and investigation of a two-component adhesive composed of soybean flour and sugar solution for plywood manufacturing. *Wood Material Science & Engineering* 17: e2086067. https://doi.org/10.1080/17480272.2022.2086067
- Zhou, C.; Li. Z.; Kaner, J.; Leng, C. 2022a. Development of a selection system for the colour of ward-robe furniture. *BioResources* 17(3): 3912-3928. https://doi.org/10.15376/biores.17.3.3912-3928
- **Zhou, C.; Shi, Z.; Kaner, J. 2022b.** Life cycle analysis for reconstituted decorative lumber from an ecological perspective: a review. *BioResources* 17(3): 4052-4063 https://doi.org/10.15376/biores.17.3.Zhou1
- Zhu, Z.; Jin, D.; Wu, Z.; Xu, W.; Yu, Y.; Guo, X.; Wang, A. 2022. Assessment of surface roughness in milling of beech using a response surface methodology and an adaptive network-based fuzzy inference system. *Machines* 10(7): e567. https://doi.org/10.3390/machines10070567